Semiclassical theory of Coulomb blockade peak heights in chaotic quantum dots

Evgenii E. Narimanov,[1] Harold U. Baranger,[2] Nicholas R. Cerruti,[3] and Steven Tomsovic[3]
[1] *Electrical Engineering Department, Princeton University, Princeton, New Jersey 08544*
[2] *Department of Physics, Duke University, Box 90305, Durham, North Carolina 27708-0305*
[3] *Department of Physics, Washington State University, Pullman, Washington 99164-2814*
(Received 7 January 2001; published 28 November 2001)

We develop a semiclassical theory of Coulomb blockade peak heights in chaotic quantum dots. Using Berry's conjecture, we calculate peak height distributions and correlation functions. We demonstrate that corrections to the corresponding results of the standard statistical theory are nonuniversal, and can be expressed in terms of the classical periodic orbits of the dot that are well coupled to the leads. The main effect is an oscillatory dependence of the peak heights on any parameter which is varied; it is substantial for both symmetric and asymmetric lead placement. Surprisingly, these dynamical effects do not influence the full distribution of peak heights, but are clearly seen in the correlation function or power spectrum. For nonzero temperature, the correlation function obtained theoretically is consistent with that measured experimentally.

DOI: 10.1103/PhysRevB.64.235329 PACS number(s): 73.23.Hk, 05.45.Mt, 73.21.−b, 73.40.Gk

I. INTRODUCTION

The Coulomb blockade is a fundamentally classical effect in microstructures—the addition of an electron to an isolated microstructure requires a certain amount of electrostatic energy, the charging energy $e^2/2C$, where C is the capacitance of the structure. It is the simplest effect of electron charge in microstructures, and has been extensively studied with regard to both fundamentals and applications in single-electron transistors.[1] One common way to study the Coulomb blockade is by measuring the conductance through a nearly isolated nanoparticle (using tunneling contacts) as a function of a gate voltage which tunes the electrostatic potential of the particle. For most values of the gate voltage, the conductance is very small, since the flow of electrons is blocked because the charging energy is not available. However, when the gate voltage is tuned so that states differing by one charge have the same energy, there is a peak in the conductance. The height of this peak is simply the conductance of the two tunnel barriers in series, and the spacing of the peaks is uniform with a separation e^2/C.

For the smallest quantum dots and at low temperature, however, quantum-mechanical interference becomes important. Interference causes variations in both the height and spacing of the conductance peaks. For the spacing, single-particle quantization and the residual interactions among the electrons are important. For the height, the nature of the wave functions become critical: if the wave function of the state at the chemical potential is poorly coupled to the leads—if it has nodes at the leads—then the conductance peak is small, but if the wave function is well coupled to the leads then the peak is large. In this paper, we restrict our attention to fluctuations in the conductance peak heights, and investigate what this tells us about wave functions in quantum dots.

Since dots are generally irregular in shape, the classical dynamics of the electrons is chaotic, and so the characteristics of Coulomb blockade peaks reflect those of wave functions in chaotic systems.[2–5] Previously, a statistical theory for the peaks was developed[2–4] by assuming these wave functions to be completely random and uncorrelated with each other. The random-matrix theory used was known to be a good description of energy-level statistics, and so likely to be reasonable for wave functions. The experimental data[6,7] for the distribution of the Coulomb blockade peak heights were found to be in excellent agreement with the predictions of the statistical theory, thus supporting the conjecture of an effective ''randomness'' of quantum dot wave functions.

A potential problem with the statistical theory was, however, evident in one of the first experiments: there is no correlation between different wave functions in random-matrix theory, so the statistical theory predicts zero correlation between neighboring conductance peaks; however in one of the experiments[7] correlation was clearly present in the form of a slowly varying envelope modulating the peak heights. In subsequent years a number of different effects were investigated as candidates to explain this correlation. The simplest of these is the effect of nonzero temperature: since excitation above the Fermi level is possible, several resonances contribute to each peak, and a given resonance contributes to several neighboring conductance peaks, inducing correlation. However, in a detailed study, this was found to be insufficient to account for the observed correlations.[8] Other explanations that were explored include correlation due to spin-paired levels,[8,9] those due to a decrease of the effective level spacing found in density-functional calculations,[10] and those due to level anticrossings in interacting many-particle systems.[11] While these latter explanations rely on subtle electron-electron interaction effects, here we argue that peak height correlations already arise within an effective single-particle picture of electrons in the quantum dot. The specific internal dynamics of the dot, even though it is chaotic, modulates the peaks: because all systems have short-time dynamical features, chaos is not equivalent to randomness.

While the statistical theory is ''universal'' in that it depends on no specific features of the quantum dot at hand, the classical dynamics in the dot is clearly not universal. Thus, while correlations between the conductance peak heights are generally present in quantum dots, the particular correlations in a given dot are not universal but rather involve detailed

information about the dot. The simplest information to include is the spatial correlation function of the wave functions—this is very short length dynamical information—and an approach including this effect was given in Ref. 12. Going beyond this, we use semiclassical techniques to derive a relation between the quantum conductance peak height and the classical periodic orbits in the dot.

The main result is that as a system parameter varies—the magnetic field, for instance, or the number of electrons in the dot (controlled by varying a gate voltage)—the interference around each periodic orbit oscillates between being destructive and constructive. When the interference is constructive for those periodic orbits which come close to the leads used to contact the dot, the wave function is enhanced near the leads, the dot-lead coupling is stronger, and so the conductance is larger. Likewise, destructive interference produces a smaller conductance. The resulting modulation at frequencies corresponding to the periodic orbits can be substantial. Because of dephasing effects, only the short periodic orbits, indeed perhaps only the shortest one, is likely to be significant.

Similar short-time dynamical effects have been noted in other contexts such as atomic and molecular spectra,[13–15] eigenfunction scarring,[15,16] magnetotransport in antidot lattices,[17] and tunneling into quantum wells.[18–21] The periodic orbit modulation that we discuss here is completely omitted in theories in which the wave function is assumed to change randomly as the system changes.[2–4] Reassuringly, the predicted dynamical modulation is of the type in the original anomalous experiment.[7] More recently, other experimental data have been published which show the effect,[9,22] but to date no systematic experimental study of this effect has been performed.

In the rest of this paper, we generalize some results previously reported in Ref. 23 to address asymmetric lead placement and to incorporate temperature dependence. The derivation given here is completely different from the previous one, which relied on the methods of Ref. 21: here our approach in terms of a statistical ansatz for the wave functions yields more results for chaotic systems, but misses the results for regular systems that we obtained previously. It has been suggested that a symmetric lead placement would not produce an observable oscillation in the average conductance,[12] but the method employed there only included spatial correlations in the wave functions and not the short-time dynamics which we consider here. In Sec. II we express the height of the conductance peak in terms of the resonant wave function. The basic ansatz for the distribution of the wave functions, including dynamical effects, is presented in Sec. III. In Sec. IV our results for the conductance peak heights are obtained. Comparison to numerical results for the stadium billiard in Sec. V confirms the adequacy of the semiclassical approach. Finally, we close with a summary and discussion of future directions.

II. HEIGHT OF A CONDUCTANCE PEAK IN COULOMB BLOCKADE

Our starting point is the connection between the Coulomb blockade peak heights and the widths of the levels in the quantum dot. This connection is well known;[24] it allows us to express the conductance in terms of single-particle quantities. We consider a dot close to two leads, so that the width Γ of a level comes from the tunneling of the electron to either lead. When the mean separation of levels is larger than the temperature T, which itself is much larger than the mean width, the electrons pass through a single quantized level in the dot, and the conductance peak height is[24]

$$G_{\rm peak}=\frac{e^2}{h}\,\frac{\pi}{2kT}\,\frac{\Gamma_1\Gamma_2}{\Gamma_1+\Gamma_2}, \tag{1}$$

where Γ_1 and Γ_2 are the partial decay widths due to the tunneling into a single lead, and spin degrees of freedom are neglected. In particular, when the leads are identical and symmetrically attached to the dot:

$$G_{\rm peak}=\frac{e^2}{h}\,\frac{\pi}{4kT}\,\Gamma_1. \tag{2}$$

The partial width is related by Fermi's golden rule to the square of the matrix element for tunneling between the lead and the dot, $M^{l\to d}$. A convenient expression for the matrix element in terms of the lead and dot wave functions, Ψ_l and Ψ_d, respectively, was derived by Bardeen,[25] and can be expressed as[18,19]

$$M^{l\to d}=\frac{\hbar^2}{m_*}\int_S d\mathbf{r}\Psi_l(\mathbf{r})\nabla\Psi_d(\mathbf{r}), \tag{3}$$

where the surface S is the edge of the quantum dot. The partial width Γ, then, depends on the square of the normal derivative of the dot wave function at the edge weighted by the lead wave function. The dot wave function Ψ_d in Eq. (3) is calculated for the effective potential, which accounts for interactions in the dot in the mean-field approximation. For the partial width we then obtain

$$\Gamma_\alpha[\Psi_d]=\frac{2\pi\hbar^4}{m_*^2}\sum_l \rho_l^{(\alpha)}\int_S d\mathbf{r}_1\cdot\nabla\Psi_d(\mathbf{r}_1) \times\int_S d\mathbf{r}_2\cdot\nabla\Psi_d(\mathbf{r}_2)^*[\Psi_l^{(\alpha)}(\mathbf{r}_1)^*\Psi_l^{(\alpha)}(\mathbf{r}_2)], \tag{4}$$

where α is the index of the lead, the integer l represents different transverse subbands in the lead, and ρ_l is the density of states in the lead for a given subband. To obtain the statistics of the conductance peak heights, we thus need to know the statistical properties of the dot wave functions Ψ_d.

III. WAVE FUNCTIONS IN THE DOT: STATISTICAL DESCRIPTION

For a *single* dot, we consider an ensemble of Coulomb blockade peaks—measured either in a narrow interval of gate voltage or obtained by following a single resonance under a continuously changing magnetic field. The wave functions associated with the peaks of the conductance will vary—or

''fluctuate''—in a way characterized by a distribution $P[\psi]$ which we seek.

It was first conjectured by Berry that the wave functions of a classically chaotic system fluctuate with certain universal properties, and can be characterized as random variables.[26] This is the foundation of the first statistical theory of peak heights.[2] Subsequently, the statistical ansatz made by Berry has been further developed. One direction of refinement is the incorporation of some short length-scale aspects of the real classical dynamics. First, a constraint of an arbitrary correlation function

$$C(\mathbf{r}_1,\mathbf{r}_2)\equiv\int \mathcal{D}\psi P[\psi]\psi^*(\mathbf{r}_1)\psi(\mathbf{r}_2) \tag{5}$$

was incorporated into the ansatz.[27,28] By using the correlation function of a random superposition of plane waves, the probability distributions of level widths and conductance peaks in the case of multimode leads to the quantum dot were found.[12,27] A distribution similar to this ansatz was derived microscopically for disordered systems, a specific kind of chaotic system, using the nonlinear sigma model.[29–32]

The next step was to constrain the correlation function by the short-time classical dynamics. Using the short-path semiclassical correlation, Srednicki and co-workers[33,34] studied correlations in chaotic eigenfunctions at large separations, and found that the predicted correlations are in excellent agreement with numerical calculations in chaotic billiards.[33] This semiclassically constrained ansatz for $P[\psi]$ is much harder to justify—certainly no derivation in disordered systems can be made. However, progress toward this goal was achieved by Kaplan and Heller by treating the nonlinear effects of classical recurrences.[16] In a recent paper by Kaplan,[35] short-time dynamics were incorporated into the general probability distribution of Ref. 27 to improve the random-matrix theory results for the conductance peak height statistics.

Here we use a maximum entropy technique[36] to derive the specific form of the distribution $P[\psi]$ that we need. An advantage of this approach is that arbitrary constraints can be introduced, as in the case of normalization which we discuss below. We make the following ansatz: the distribution $P[\psi]$ maximizes the information entropy[37]

$$H=-\int \mathcal{D}\psi\, P[\psi]\log P[\psi] \tag{6}$$

within the space allowed by the constraints. Here the measure corresponding to the distribution $P[\psi]$ is defined in the standard way,[34]

$$\mathcal{D}\psi_d=\lim_{N\to\infty}\Pi_{n=1}^{N} d\psi_d(\mathbf{r}_n), \tag{7}$$

so that the product $P[\psi_d]\mathcal{D}\psi_d$ represents the probability that a wave function $\psi(\mathbf{r})$ of the original ensemble is between $\psi_d(\mathbf{r})$ and $\psi_d(\mathbf{r})+d\psi_d(\mathbf{r})$ for any point $\mathbf{r}$ inside the dot.

Assuming that the *only* constraint imposed on the ensemble of wave functions is the correlation function $C(\mathbf{r}_1,\mathbf{r}_2)$, the maximum of functional (6) under constraint (5) is equivalent to the extremum of the functional

$$F[\psi]=\int \mathcal{D}\psi\Big[-P[\psi]\log P[\psi]-\int d\mathbf{r}_1\int d\mathbf{r}_2\lambda(\mathbf{r}_1,\mathbf{r}_2) \times\{\psi^*(\mathbf{r}_1)\psi(\mathbf{r}_2)P[\psi]-C(\mathbf{r}_1,\mathbf{r}_2)\}\Big], \tag{8}$$

where the Lagrange multiplier $\lambda(\mathbf{r}_1,\mathbf{r}_2)$ can then be determined from Eq. (5). Setting the first variation of $F[\psi]$ equal to zero, we find that $P[\psi]$ is Gaussian. The final result, obtained by substituting Eq. (5) to find $\lambda(\mathbf{r}_1,\mathbf{r}_2)$, is

$$P[\psi]=A\exp\Big[-\frac{\beta}{2}\int d\mathbf{r}_1\int d\mathbf{r}_2\psi^*(\mathbf{r}_1)C^{-1}(\mathbf{r}_1,\mathbf{r}_2)\psi(\mathbf{r}_2)\Big], \tag{9}$$

where A is the normalization [independent of $\psi(\mathbf{r})$], and C^{-1} is the functional inverse of the two-point correlation function $C(\mathbf{r}_2,\mathbf{r}_1|\varepsilon)$

$$\int d\mathbf{r}_3 C^{-1}(\mathbf{r}_1,\mathbf{r}_3)C(\mathbf{r}_3,\mathbf{r}_2)=\delta(\mathbf{r}_1-\mathbf{r}_2). \tag{10}$$

The coefficient $\beta=1$ for a system with time-reversal invariance, when the wave functions can be chosen real, and $\beta=2$ otherwise.

It has been shown[34] that in the small-$\hbar$ limit for classically chaotic systems, the correlation function $C(\mathbf{r}_2,\mathbf{r}_1)$ can be expressed in terms of the semiclassical approximation to the Green function[13] $G_{\rm sc}(\mathbf{r}_2,\mathbf{r}_1)$ as

$$C(\mathbf{r}_2,\mathbf{r}_1)=\frac{1}{\pi\overline{\rho}_{\rm sc}}\mathrm{Im}G_{\rm sc}(\mathbf{r}_2,\mathbf{r}_1)+O(\hbar^{3/2}) \tag{11}$$

where $\overline{\rho}_{\rm sc}(\varepsilon)$ is the smooth part of the density of states (DOS) in the dot, given by the leading order (Thomas-Fermi) semiclassical approximation to the DOS.

In the semiclassical approximation, the energy-averaged Green function can be expressed in terms of the classical trajectories (labeled by the index j)[13,38]

$$G_{\rm sc}(\mathbf{r}_2,\mathbf{r}_1)=G_0(\mathbf{r}_2,\mathbf{r}_1)+\frac{1}{i\hbar}\frac{1}{\sqrt{2\pi i\hbar}}\sum_j\sqrt{|D_j|} \times\exp\Big(i\frac{S_j}{\hbar}-in_j\frac{\pi}{4}\Big)\exp\Big(-\frac{\tau_j^2W^2}{2\hbar^2}\Big), \tag{12}$$

where $S_j=S_j(\mathbf{r}_2,\mathbf{r}_1)$ is the classical action, τ_j is the period, the integer n_j is the topological index[13] of the trajectory j, and the amplitude D_j is

$$D_j=\det\begin{pmatrix}\dfrac{\partial^2S_j(\mathbf{r}_2,\mathbf{r}_1)}{\partial\mathbf{r}_2\partial\mathbf{r}_1} & \dfrac{\partial^2S_j(\mathbf{r}_2,\mathbf{r}_1)}{\partial\varepsilon\,\partial\mathbf{r}_1}\\ \dfrac{\partial^2S_j(\mathbf{r}_2,\mathbf{r}_1)}{\partial\varepsilon\,\partial\mathbf{r}_2} & \dfrac{\partial^2S_j(\mathbf{r}_2,\mathbf{r}_1)}{\partial\varepsilon^2}\end{pmatrix}. \tag{13}$$

We have specialized to two spatial dimensions and the last exponential in Eq. (12) is due to a Gaussian averaging over an energy window of width W described below. The function $G_0(\mathbf{r}_2,\mathbf{r}_1)$ is the contribution of the nonclassical so-called

''zero-length'' trajectories, those with actions less than or of order $\hbar$. Therefore, $G_0(\mathbf{r}_2,\mathbf{r}_1)$ cannot be obtained using the stationary-phase approximation, but may be evaluated[26,34] by replacing the actual propagator $\langle \mathbf{r}_2|\exp(-iHt/\hbar)|\mathbf{r}_1\rangle$ by its free-space analog

$$\langle \mathbf{r}_2|\exp\left(-\frac{iHt}{\hbar}\right)|\mathbf{r}_1\rangle \approx \int \frac{d\mathbf{p}}{(2\pi\hbar)^2}\exp\left(i\frac{\mathbf{p}(\mathbf{r}_2-\mathbf{r}_1)}{\hbar}\right) \times \exp\left(-\frac{iH(\mathbf{p},\mathbf{r}_0)t}{\hbar}\right) \tag{14}$$

where $\mathbf{r}_0 \equiv (\mathbf{r}_2+\mathbf{r}_1)/2$. The corresponding Green function is then

$$G_0(\mathbf{r}_2,\mathbf{r}_1) = \int \frac{d\mathbf{p}}{(2\pi\hbar)^2}\exp\left(i\frac{\mathbf{p}\cdot(\mathbf{r}_2-\mathbf{r}_1)}{\hbar}\right)\frac{1}{\varepsilon - H(\mathbf{p},\mathbf{r}_0)+i0}. \tag{15}$$

Note that because of the short trajectory involved, this part of the Green function varies very smoothly as a function of energy. The smooth part of the correlation function which results is

$$C_0(\mathbf{r}_2,\mathbf{r}_1) = \frac{1}{=\!\!=\!\!\rho_{sc}}\int \frac{d\mathbf{p}}{(2\pi\hbar)^2}\cos\left(\frac{\mathbf{p}(\mathbf{r}_2-\mathbf{r}_1)}{\hbar}\right)\delta[\varepsilon - H(\mathbf{p},\mathbf{r}_0)], \tag{16}$$

and so $C_0(\mathbf{r}_2,\mathbf{r}_1) \propto J_0(p|\mathbf{r}_2-\mathbf{r}_1|/\hbar)$. This smooth part of the correlation function is rather local in that it decays monotonically with separation. Thus, having fully specified the correlation function we wish to use, we finally obtain

$$P(\psi_d|\varepsilon) \sim \exp\left[-\frac{\beta}{2}\int d\mathbf{r}_1\int d\mathbf{r}_2\psi^* \times(\mathbf{r}_1)G_{sc}^{-1}(\mathbf{r}_2,\mathbf{r}_1|\varepsilon)\psi(\mathbf{r}_2)\right]. \tag{17}$$

A few remarks are required about the width of the energy window W. In the semiclassical limit there arises an increasingly broad separation between the short-time dynamics that give rise to system specific behavior and the long orbits that are responsible for generating universal statistical fluctuations.[16] The width W is chosen such that the short periodic orbits are included in the sum essentially undamped, whereas the long orbits are eliminated since their contributions are already accounted for in the statistical ansatz. For the rest of this paper, we will eliminate the explicit dependence on W and the sum is understood to contain only the linear dynamics.

The general ensemble defined by distribution (9) has, however, certain limitations. Strictly speaking, in its general form this ensemble is only suitable for calculations of those observables which can be represented in terms of only two-point products $\psi^*(\mathbf{r}_1)\psi(\mathbf{r}_2)$. The reason for this problem is as follows: instead of the proper normalization of *each member of the ensemble*,

$$\int d\mathbf{r}|\psi(\mathbf{r})|^2 = 1, \tag{18}$$

the normalization of the wave functions is satisfied *only on average*:

$$\int \mathcal{D}\psi(\mathbf{r})P[\psi(\mathbf{r})]\int d\mathbf{r}|\psi(\mathbf{r})|^2 = 1. \tag{19}$$

As a result, the higher-order moments $\Delta_n \equiv \langle \int d\mathbf{r}_1 \ldots \int d\mathbf{r}_n|\psi(\mathbf{r}_1)|^2 \ldots |\psi(\mathbf{r}_n)|^2\rangle_\psi$ of the distribution are different from unity. Therefore, in its general from, the ensemble defined by Eq. (9) is not suitable for calculations which are sensitive to the $n>1$ moments of the distribution $P[\psi]$, such as for the description of the residual interactions in quantum dots.[39–41]

The method developed in this section yields a straightforward way to generalize distribution (9) to properly account for the higher moments. For example, adding an additional constraint

$$\int \mathcal{D}\psi P[\psi]\int d\mathbf{r}_1\int d\mathbf{r}_2|\psi(\mathbf{r}_1)|^2|\psi(\mathbf{r}_2)|^2 = 1, \tag{20}$$

to the variational problem [Eq. (6)] will yield a generalization of distribution (17) which properly accounts for the moment Δ_2.

Note, in contrast, that the errors in the higher moments, $n>1$, produced by the *semiclassical* distribution [Eq. (17)] are of higher order in $\hbar$, $\delta_n \sim O(\hbar^2)$ than the terms taken into account in G_{sc}.[42] As long as these higher-order corrections are not relevant for the quantity under consideration, one can generally use the *semiclassical* distribution [Eq. (17)].

IV. PEAK HEIGHT DISTRIBUTION

Since the Coulomb blockade peak heights are uniquely determined by the corresponding dot wave functions ψ_d, the peak heights distribution function $P(G)$ is given by

$$P(G) = \int \mathcal{D}\psi_d P(\psi_d)\delta(G - G_{\text{peak}}[\psi_d]), \tag{21}$$

where $G_{\text{peak}}[\psi]$ is determined by Eqs. (1), (2), and (4). The width Γ depends only on the wave function near the boundary of the quantum dot, as follows from Eq. (4). If the function $P_S(\overline{\psi})$ represents the distribution of the wave functions in a narrow strip S along the boundary of the quantum dot, so that

$$\psi(\mathbf{r}) = \begin{cases} \overline{\psi}(\mathbf{r}), & \mathbf{r}\in S \\ \hat{\psi}(\mathbf{r}), & \mathbf{r}\notin S, \end{cases} \tag{22}$$

then the conductance distribution is

$$P(G) = \int \mathcal{D}\overline{\psi}\, P_S[\overline{\psi}|\varepsilon]\,\delta(G - G_{\text{peak}}[\overline{\psi}]). \tag{23}$$

The ''edge'' distribution P_S can be obtained from the general distribution $P[\psi]$ by integrating out the values of $\hat{\psi}$:

$$P_S[\bar{\psi}]=\int \mathcal{D}\hat{\psi}P[\psi\{\bar{\psi},\hat{\psi}\}]. \tag{24}$$

As the distribution $P[\psi]$ is Gaussian, the resulting functional integral can be calculated exactly, yielding

$$P_S[\bar{\psi}]=A_S\exp\left[-\frac{\beta}{2}\int_S d\mathbf{q}_1\int_S d\mathbf{q}_2\bar{\psi}^*(\mathbf{q}_1)\bar{K}(\mathbf{q}_1,\mathbf{q}_2)\bar{\psi}(\mathbf{q}_2)\right], \tag{25}$$

where

$$\bar{K}(\mathbf{q}_1,\mathbf{q}_2)=C^{-1}(\mathbf{q}_1,\mathbf{q}_2)+\int_{\Omega\setminus S}d\mathbf{q}_3\int_{\Omega\setminus S}d\mathbf{q}_4 \times C^{-1}(\mathbf{q}_1,\mathbf{q}_3)C(\mathbf{q}_3,\mathbf{q}_4)C^{-1}(\mathbf{q}_4,\mathbf{q}_2) \tag{26}$$

and A_S is the new normalization constant. The spatial integrals are over the part of the total space Ω which is orthogonal to the edge S, denoted $\Omega\setminus S$.

As follows from Eqs. (11) and (12), the ''nondiagonal'' part of the correlation function is of a higher order in $\hbar$, $\sim O(\sqrt{\hbar})$, compared to the ''diagonal'' part $C_0\sim O(1)$. The second term in Eq. (26) involves the correlation functions $C(\mathbf{q}_1,\mathbf{q}_3)$ and $C(\mathbf{q}_4,\mathbf{q}_2)$, taken between the points of the *different* parts of the dot—the edge strip S for one coordinate and the internal region $\Omega\setminus S$ for the other. It is therefore of higher order in $\hbar$, $\sim\mathcal{O}(\hbar)$, than the first contribution, $C^{-1}(\mathbf{q}_1,\mathbf{q}_2)\sim\delta(\mathbf{q}_2-\mathbf{q}_1)O(1)+O(\sqrt{\hbar})$. Keeping such higher-order terms is not consistent with the leading-order semiclassical approximation we used for $C(\mathbf{q}_1,\mathbf{q}_2)$. We therefore obtain

$$P_S[\bar{\psi}]=A_S\exp\left[-\frac{\beta}{2}\int_S d\mathbf{q}_1\int_S d\mathbf{q}_2\bar{\psi}^*(\mathbf{q}_1) \times C^{-1}(\mathbf{q}_1,\mathbf{q}_2)\bar{\psi}(\mathbf{q}_2)\right]. \tag{27}$$

An alternative to the argument given here proceeds by noting that integrating out $\hat{\psi}$ should yield a Gaussian in $\bar{\psi}$, and that this Gaussian, by construction of the ensemble, must reproduce the correct two point correlation function $C(\mathbf{q}_1,\mathbf{q}_2)$. This alternative argument[28] yields immediately the functional form [Eq. (27)].

When the *closed* dot is defined by the Dirichlet boundary conditions, the wave function in the narrow strip S near the ''edge'' can be represented as

$$\bar{\psi}=z\varphi(y), \tag{28}$$

where y is the coordinate along the boundary of the dot, and z is in the direction of the normal. In this limit, the correlation function is

$$C(\mathbf{q}_1,\mathbf{q}_2)=z_2z_1\partial_nC(y_1,y_2), \tag{29}$$

where $\partial_nC(y_1,y_2)$ is defined as the correlation function of the normal derivatives of the wave function at the boundary of the dot and can be obtained as

$$\partial_nC(y_2,y_1)=\frac{1}{\pi\bar{\rho}_{\rm sc}}\mathrm{Im}\partial_nG_{\rm sc}(y_2,y_1)+O(\hbar^{(d+1)/2}), \tag{30}$$

where

$$\partial_nG(y_2,y_1|\varepsilon)\equiv\sum_m\frac{\partial_n\psi_m^*(y_2,0)\partial_n\psi_m(y_1,0)}{\varepsilon_m-\varepsilon+i0}. \tag{31}$$

The semiclassical approximation $\partial_nG_{\rm sc}$ for the normal derivative Green function was derived in Ref. 21,

$$\partial_nG_{\rm sc}(y_2,y_1)=\partial_nG_0(y_2,y_1)+\frac{4}{i\hbar^3}\frac{1}{\sqrt{2\pi i\hbar}} \times\sum_j[\mathbf{p}_j(y_1)]_n[\mathbf{p}_j(y_2)]_n\sqrt{|D_j|} \times\sin\left(\frac{S_j}{\hbar}-\bar{n}_j\frac{\pi}{4}\right), \tag{32}$$

where $\bar{n}_j$ and $[\mathbf{p}_j]_n$ are, respectively, the Maslov indexes[13] and the normal component of the classical momentum of the trajectory j.

In order to connect the dot wave functions to the lead, let $\{\phi_m(y)\}$ be the complete orthogonal set of the wave functions corresponding to the transverse potential of the lead. Using this basis, we represent the function $\varphi(y)$ as

$$\varphi(y)=\sum_{m=0}^{\infty}a_m\phi_m(y-y_l), \tag{33}$$

where y_l is the contact point of the lead. Assuming that the tunneling between the lead and the dot is dominated by the contribution of the lowest transverse subband of the lead, and using Eq. (4) for the partial width Γ_α, we obtain

$$\Gamma_\alpha=2\pi\rho_0^{(\alpha)}\left(\frac{\hbar^2}{m_*}\right)^2\left|\int dy\,\phi_0(y)\sum_m a_m\phi_m(y)\right|^2 =\frac{2\pi\hbar^4}{m_*^2}\rho_0^{(\alpha)}|a_0|^2, \tag{34}$$

where $\rho_0^{(\alpha)}$ is the density of states in the lead corresponding to the lowest transverse subband. For an arbitrary moment of the partial width $\langle\Gamma_\alpha^m\rangle$, we therefore find

$$\langle\Gamma_\alpha^m\rangle\propto\int da_0\left[\frac{2\pi\hbar^4}{m_*^2}\rho_0^{(\alpha)}\right]^m|a_0|^{2m}\exp\left[-|a_0|^2 \times\int dy_1\int dy_2\phi_0(y_1)\frac{1}{\partial_nC(y_1,y_2)}\phi_0(y_2)\right]. \tag{35}$$

To give explicit expressions for the distribution of level widths and conductance, we specialize to the time-reversal symmetric case ($\beta=1$, GOE) for the rest of this paper; the case, when time-reversal symmetry is broken by a magnetic

field ($\beta=2$, GUE), can be treated in an analogous way. In the presence of time-reversal symmetry, the wave functions, and hence the coefficient a_0, can be chosen real, yielding

$$\langle\Gamma^m\rangle\propto\int d\Gamma\,\Gamma^m\frac{\exp(-\Gamma/2\bar{\Gamma})}{\sqrt{\Gamma}}, \tag{36}$$

where

$$\bar{\Gamma}=\frac{\hbar^4}{m_*^2}\frac{\rho_0^{(\alpha)}}{\bar{\rho}_{\rm sc}}\times\left(\int dy_1\int dy_2\,\phi_0(y_1)\frac{1}{\mathrm{Im}[\partial_n G_{\rm sc}(y_2,y_1|\varepsilon)]}\phi_0(y_2)\right)^{-1}. \tag{37}$$

Thus the partial width is characterized by the Porter-Thomas distribution

$$P(\Gamma)\propto\frac{1}{\sqrt{\Gamma}}\exp\left(-\frac{\Gamma}{2\bar{\Gamma}}\right), \tag{38}$$

with the slowly varying local average $\bar{\Gamma}(\varepsilon)$. This explicit result for the distribution of level widths is the main result of this section.

The conductance distribution $P(G)$ can now be simply derived in two limiting cases: (i) when the leads are placed symmetrically, so that $\Gamma_1=\Gamma_2$ [cf. Eq. (2)], and (ii) when one of the partial widths is substantially smaller than the other, $\Gamma_1\ll\Gamma_2$. In both these cases $G\sim\Gamma_1$ [as follows from Eq. (1)], and the conductance distribution is also of Porter-Thomas type. The ''local average'' conductance $\bar{G}$ is given by

$$\bar{G}(\varepsilon)=\frac{e^2\pi}{2\gamma hkT}\bar{\Gamma}(\varepsilon), \tag{39}$$

where the ''local average'' width $\bar{\Gamma}(\varepsilon)$ is defined by Eq. (37), and $\gamma=1$ for $\Gamma_1\ll\Gamma_2$, while $\gamma=2$ for $\Gamma_1=\Gamma_2$.

In the general case, $\Gamma_1/\Gamma_2\sim O(1)$ but not identical, however, an exact calculation of the conductance distribution is complicated by the essentially nonlinear dependence of the conductance on the partial widths Γ_1 and Γ_2. In order to calculate the actual conductance, we choose the area S as the composition of two narrow strips S_1 and S_2 near each of the leads. Using the transverse lead wave functions as the basis in each of the two strips,

$$\bar{\psi}(y,z)=z\left[\sum_m a_m^{(1)}\phi_m^{(1)}(y-y_l^{(1)})+\sum_m a_m^{(2)}\phi_m^{(2)}(y-y_l^{(2)})\right], \tag{40}$$

where the coordinates $y_l^{(1)}$ and $y_l^{(2)}$ represent the ''contact points'' of the leads. The partial widths Γ_1 and Γ_2 are then given by

$$\Gamma_1=\frac{2\pi\hbar^4}{m_*^2}\rho_0^{(1)}|a_0^{(1)}|^2, \tag{41}$$

$$\Gamma_2=\frac{2\pi\hbar^4}{m_*^2}\rho_0^{(2)}|a_0^{(2)}|^2. \tag{42}$$

Assuming an equal density of states in the leads, $\rho_0^{(1)}(\varepsilon)=\rho_0^{(2)}(\varepsilon)$, for the conductance G we obtain

$$G=\frac{\pi}{2}\frac{e^2\hbar^3}{m_*^2kT}\rho_0\frac{|a_0^{(1)}|^2|a_0^{(2)}|^2}{|a_0^{(1)}|^2+|a_0^{(2)}|^2}. \tag{43}$$

An arbitrary nth moment of the conductance G, $\langle G^n\rangle$, can now be calculated by integrating over the coefficients $\{a_m\}$ for $m\neq 0$, yielding

$$\langle G^n\rangle\propto\int da_0^{(1)}\int da_0^{(2)}\left[\frac{|a_0^{(1)}|^2|a_0^{(2)}|^2}{|a_0^{(1)}|^2+|a_0^{(2)}|^2}\right]^n\exp[-a_0^{(1)}\mathcal{A}_{11}a_0^{(1)}-a_0^{(2)}\mathcal{A}_{22}a_0^{(2)}-2a_0^{(1)}\mathcal{A}_{12}a_0^{(2)}], \tag{44}$$

where the matrix $\mathcal{A}$ is

$$\mathcal{A}_{\alpha\beta}=\int dy_1\int dy_2\,\phi_0(y_1-y_l^{(\alpha)})\partial_n C^{-1}(y_1,y_2)\times\phi_0(y_2-y_l^{(\beta)}). \tag{45}$$

Note that definition (45) implies that the diagonal elements of the matrix $\mathcal{A}$ are proportional to the corresponding partial widths, $\mathcal{A}_{11}\sim\Gamma_1$, $\mathcal{A}_{22}\sim\Gamma_2$. A straightforward evaluation of the integrals in Eq. (44) using the substitution

$$x=[a_0^{(1)}]^2-\frac{2m_*^2kTG}{\pi e^2\hbar^3\rho_0}, \tag{46}$$

yields

$$\langle G^n\rangle=\int dG\,G^nP(G), \tag{47}$$

where the distribution is

$$P(G)=\frac{1}{\sqrt{G}}\exp\left(-\frac{1}{2}\mathrm{Tr}\mathcal{A}G\right)\int_0^\infty dx\,\frac{G+x}{x^{3/2}}\exp\left[-\frac{1}{2}\mathcal{A}_{11}x-\frac{1}{2}\mathcal{A}_{22}\frac{G^2}{x}\right]\cosh\left[\mathcal{A}_{12}G\left(\sqrt{\frac{x}{G}}+\frac{G}{x}\right)\right]. \tag{48}$$

Note that it is only the term involving $\mathcal{A}_{12}$ which makes the remaining integral non-Gaussian and so, thus hard to perform. However, this term is semiclassically small: from Eq. (45) it follows that the leading semiclassical term in the off-diagonal part of the matrix $\mathcal{A}$ is of next order in $\hbar$ compared to the leading diagonal terms. The x integral in Eq. (48) is therefore dominated by the interval between $1/(G\mathcal{A}_{11})$ and $G\mathcal{A}_{22}$, where the off-diagonal matrix element $\mathcal{A}$ makes only a small correction *quadratic* in $\mathcal{A}_{12}$. Such a correction corresponds, however, to higher-order terms in $\hbar$. Corrections of this order were already neglected in the original semiclassical expansion of the Green function, and so to be consistent we discard all effects of the off-diagonal matrix element $\mathcal{A}_{12}$ here. The integral in Eq. (48) can now be easily performed.

The semiclassical approximation to the conductance distribution is, then, simply a Porter-Thomas distribution, even in the general case,

$$P(G)=\left(\frac{2\pi}{\overline{G}}\right)^{1/2}\frac{1}{\sqrt{G}}\exp\left[-\frac{G}{2\overline{G}}\right], \tag{49}$$

where the ''local average'' conductance $\overline{G}$ is

$$\overline{G}\equiv\left[\frac{1}{\sqrt{\overline{G}_1}}+\frac{1}{\sqrt{\overline{G}_2}}\right]^{-2}, \tag{50}$$

and the ''partial conductance'' G_α is related to the partial width Γ_α via the standard relation

$$G_\alpha\equiv(\pi e^2/2hkT)\Gamma_\alpha. \tag{51}$$

As the semiclassical Green function, $G_{\rm sc}$, and, consequently, the correlator, $\partial_n C$, can be expressed as a sum of the contributions of ''zero-length'' and longer classical trajectories, similar decompositions hold for the average partial width and average partial conductance:

$$\overline{\Gamma}_\alpha=\overline{\Gamma}^0_\alpha+\overline{\Gamma}^{\rm osc}_\alpha, \tag{52}$$

$$\overline{G}_\alpha=\overline{G}^0_\alpha+\overline{G}^{\rm osc}_\alpha, \tag{53}$$

where the ''oscillatory'' parts $\overline{\Gamma}^{\rm osc}$ and $\overline{G}^{\rm osc}$ depend on the longer classical trajectories and are of next order in $\hbar$ compared to the smooth contributions $\overline{\Gamma}^0$ and $\overline{G}^0$, which are zero-length contributions. A consistent semiclassical approximation, as in Eq. (12), then requires expanding $\overline{G}$ and keeping only the linear terms in the oscillatory contribution. We thus obtain

$$\overline{G}=\frac{\overline{G}^0_1\overline{G}^0_2}{\overline{G}^0_1+\overline{G}^0_2+2\sqrt{\overline{G}^0_1\overline{G}^0_2}}\left[1+\frac{1}{1+\sqrt{\overline{G}^0_1/\overline{G}^0_2}}\frac{\overline{G}^{\rm osc}_1}{\overline{G}^0_1}+\frac{1}{1+\sqrt{\overline{G}^0_2/\overline{G}^0_1}}\frac{\overline{G}^{\rm osc}_2}{\overline{G}^0_2}\right]. \tag{54}$$

Note that in the asymmetric lead case, if the mean of the partial conductances are the same ($\overline{G}^0_1\approx\overline{G}^0_2$), then the average conductance is one-fourth the average of the partial conductances. This result differs from the completely symmetric case given in Ref. 23, where the average conductance is one-half the average partial conductances. The difference is due to the perfect correlation of the widths in the symmetric case whereas the mean may be equal in the asymmetric case, but the particular values are uncorrelated.

We now proceed to the semiclassical calculation of the ''local average'' partial width $\overline{\Gamma}$. The defining equation (37) involves the functional inverse of the Green function, which is a hard object to calculate. Instead, we will use the original definition [Eq. (4)], which for the local average partial width yields

$$\overline{\Gamma}=\frac{2\pi\hbar^4}{m_*^2}\sum_\alpha\rho_0^{(\alpha)}\int dy_1\int dy_2\,\phi_\alpha(y_1-y_l)\times\phi^*_\alpha(y_2-y_l)\partial_n C(y_1,y_2), \tag{55}$$

where the correlation function of the normal derivatives of the dot wave functions $\partial_n C(y_1,y_2)$ is related to the semiclassical Green function by Eq. (30).

If we now use some information about the lead wave functions, we can obtain an explicit expression for the average width $\overline{\Gamma}$ in terms of the classical dynamics in the dot. When, as we assumed above, the tunneling from the lead to the dot is dominated by the lowest transverse energy subband in the constriction between the lead and the dot,[3] the transverse potential in the tunneling region can be taken to be quadratic: $U_l\sim\kappa(y-y_l)^2$. In this case, the transverse dependence of the lead wave function is simply a harmonic-oscillator wave function, so that at the edge of the dot $\phi_0\simeq c_l\exp[-(y-y_l)^2/2a_{\rm eff}^2]$, where y_l is the center of the lead and constriction, and the effective width is $a_{\rm eff}=\sqrt{\hbar}/\sqrt[4]{2\kappa m^*}$. While the exact form of the lead wave function is not crucial, the $\hbar$ dependence of the width is important for the semiclassical argument which follows; note that $a_{\rm eff}\sim\sqrt{\hbar}$ does not depend on a particular transverse potential.

Using this information about ϕ_0 in the expression for the diagonal matrix elements $\mathcal{A}_{11}$, and $\mathcal{A}_{22}$, we see that the lead wave function restricts the integration to a semiclassically narrow region of width $a_{\rm eff}\sim\sqrt{\hbar}$. This allows one to express the contribution of the open trajectories entering the Green function in terms of an expansion near their closed neighbors,

$$\overline{\Gamma}=\overline{\Gamma}_0+\frac{16}{m^*}\int dy\int dp_y f_W(y,p_y)\sum_\alpha\sqrt{\frac{(p_i^\alpha)_n(p_f^\alpha)_n}{m_{11}^\alpha+m_{22}^\alpha+2}}\times\exp\left[-\frac{i}{\hbar}\frac{2m_{12}^\alpha}{m_{11}^\alpha+m_{22}^\alpha+2}(p_y-\overline{p}_y^\alpha)^2\right]\times\exp\left[i\frac{S_\alpha(y,0;y,0;\varepsilon)}{\hbar}\right], \tag{56}$$

where $\overline{\Gamma}_0$ is the monotonic part of the resonance width, $(p_i)_n$ and $(p_f)_n$ are the normal components of the initial and the final momenta of the closed orbit α, the momentum $\overline{\mathbf{p}}\equiv(\mathbf{p}_i+\mathbf{p}_f)/2$, and the 2×2 monodromy matrix[13] $M_\alpha\equiv(m_{ij}^\alpha)$ is defined via the linearization of the Poincaré map near the closed orbit α and calculated at the contact point near the lead. In Eq. (56) we have also introduced the Wigner transform f_W^e of the lead wave function,

$$f_W^e(y,p_y)\equiv h^{-1}\int d\Delta y\;\phi_0(y-\Delta y/2,0)\,\phi_0^*\times(y+\Delta y/2,0)\exp(ip_y\Delta y/\hbar), \tag{57}$$

which describes the distribution in transverse position and momentum of electrons tunneling into the dot.

In leading order in the distance between the contact point y of the closed orbit α, and the center of the lead y_l, the action of the closed orbit S_α scales linearly,

$$S_\alpha(y,0;y,0) \propto S(y_l,0;y_l,0) + \Delta p_y^\alpha (y - y_l) \tag{58}$$

where Δp_y is the change of transverse momentum after the traversal of the closed orbit. Assuming, e.g., a Gaussian form of the lead wave function, the contribution of each of these closed orbits is suppressed by a factor exponentially small in Δp_y^2. This suppression is the effect of the mismatch of the closed orbit (momentum) with the distribution of transverse momentum at the lead, which is centered at zero with width $\delta p_l \sim \hbar/a_{\rm eff} \sim \sqrt{\hbar}$ for the lowest subband. Therefore, only closed orbits with *semiclassically* small momentum change Δp contribute to the width. This in turn implies that the closed orbit is located semiclassically close (within a distance $\sim\sqrt{\hbar}$) to a *periodic orbit* for which $\Delta p \equiv 0$. Using this proximity to a periodic orbit, we can re-express the actions and momenta of the injection orbits in terms of the properties of their periodic neighbors (labeled by the index μ) as follows:

$$S_\alpha(y,0;y,0) \simeq S_\mu + \frac{\mathrm{Tr}[M_\mu]-2}{2m_{12}^\mu}(y-y_\mu)^2, \tag{59}$$

$$\overline{p_y^\alpha} \simeq p_y^\mu + \frac{m_{11}^\mu - m_{22}^\mu}{2m_{12}^\mu}(y-y_\mu). \tag{60}$$

Substitution of Eqs. (59) and (60) into Eq. (56), and integration over y, yields[23]

$$\overline{\Gamma} = \overline{\Gamma}_0 + \sum_{\mu:\mathrm{p.o.}} A_\mu \cos\left(\frac{S_\mu}{\hbar} + \phi_\mu\right), \tag{61}$$

where the monotonic part is

$$\overline{\Gamma}_0 = \frac{\sqrt{\pi}}{2} c_l^2 a_{\rm eff} \frac{p^2}{m^*} e^{-\zeta}[I_0(\zeta) + I_1(\zeta)], \quad \zeta = \frac{p^2 a_{\rm eff}^2}{2\hbar^2}, \tag{62}$$

the amplitude is

$$A_\mu = 4\sqrt{2}\,\frac{\hbar c_l^2 p_z^\mu}{m^*}[\mathrm{Tr}^2[M_\mu](1+\sigma_+^2)(1+\sigma_-^2)]^{-1/4} \times \exp\left(-\frac{\sigma_+^2 \overline{p}^2}{(1+\sigma_+^2)} - \frac{\sigma_-^2 \overline{y}^2}{(1+\sigma_-^2)}\right), \tag{63}$$

with

$$\sigma_\pm \equiv \tfrac{1}{2}[\overline{m}_{12} - \overline{m}_{21} \pm \sqrt{(\overline{m}_{22} - \overline{m}_{11})^2 + (\overline{m}_{21} + \overline{m}_{12})^2}],$$

$$\overline{m}_{ij} \equiv \frac{2m_{ij}^\mu}{\mathrm{Tr}[M_\mu]+2}\left(\frac{a_{\rm eff}^2}{\hbar}\right)^{(j-i)/2}$$

$$\theta \equiv \frac{1}{2}\arctan\left(\frac{\overline{m}_{22} - \overline{m}_{11}}{\overline{m}_{21} + \overline{m}_{12}}\right), \tag{64}$$

$$\overline{y} \equiv \cos\theta (y_\mu - y_l)/a_{\rm eff} + \sin\theta\, p_y^\mu a_{\rm eff}/\hbar,$$

$$\overline{p} \equiv \cos\theta\, p_y^\mu a_{\rm eff}/\hbar - \sin\theta (y_\mu - y_l)/a_{\rm eff},$$

and ϕ_μ is a slowly varying phase. Here I_n is the Bessel function of complex argument, p is the magnitude of the electron momentum, $\mathbf{p}^\mu$ is the electron momentum for the periodic orbit μ at the bounce point (turning point), y_μ is the bounce point coordinate, S_μ is the action of the periodic orbit, and $M_\mu \equiv (m_{ij})^\mu$ is the corresponding monodromy matrix.[13] Note the sharp suppression of the oscillatory effects in Eq. (63) if the periodic orbit does not match up to the lead wave function in *both* position and momentum space. The mismatch is characterized by $\overline{y}$ and $\overline{p}$; the most favorable case is that of a perpendicular periodic orbit hitting the edge of the dot right at the center of the lead, $p_y^\mu = 0$ and $y_\mu = y_l$, so that $\overline{y} = \overline{p} = 0$.

An explicit expression for the average conductance follows from the relation between the partial width and the partial conductance [Eq. (51)]. Using Eq. (54), we see that $\overline{G}$ can be written in the form

$$\overline{G} = \overline{G}_0 + \sum_{\mu:\mathrm{p.o.}} B_\mu \cos\left(\frac{S_\mu}{\hbar} + \phi_\mu\right), \tag{65}$$

where B_μ is simply related to A_μ, $\overline{G}_1^0$, and $\overline{G}_2^0$. This, together with Eq. (49), defines both the average conductance and its fluctuations. The oscillating form of this result is the same as that in Ref. 23, which was derived using a different approach; in fact, (61) of the present paper is identical to Eq. (3) of Ref. 23. Both approaches are systematic semiclassical approximations, and so the similarity of the two results is not surprising. It is, however, important to realize that the main objective of the present paper is to characterize both the dynamical effect in the conductance *and* the peak height distribution, while Ref. 23 dealt only with the former issue.

A further characterization of the peak fluctuations can be obtained from the peak-to-peak correlation function: this is a particularly interesting quantity because of the correlations sometimes observed experimentally,[6,7] as discussed in Sec. I. A natural measure of the statistics of nearby peaks is given by $\delta G(E_m) \equiv G(E_m) - \langle G(E_n)\rangle_n$, in terms of which the correlation function is

$$\mathrm{Corr}_m[\delta G, \delta G] = \langle \delta G(E_{n+m})\,\delta G(E_n)\rangle_n / \langle [\delta G(E_n)]^2\rangle_n. \tag{66}$$

Substituting the conductance distribution [Eq. (49)] into Eq. (66), we obtain

$$\mathrm{Corr}_m = \delta_{m,0} + (1-\delta_{m,0}) \times \frac{\sum_\mu B_\mu^2 \cos\left(\frac{\tau_\mu \Delta}{\hbar} m\right)}{4\overline{G}_0^2 + 3\sum_\mu B_\mu^2}. \tag{67}$$

Throughout this paper we have concentrated on the energy (or equivalently the peak number) as the tuning parameter causing the peak height variation. This is just an ex-

ample: exactly analogous considerations apply to any parameter causing changes in the wave functions of the quantum dot. In particular, a similar oscillatory behavior is expected in the height of a *given* peak as a function of magnetic field, often the most experimentally accessible parameter. As the field varies, the change in the action of a periodic orbit is proportional to the (directed) area that it encloses. Thus the peak heights should exhibit an oscillatory envelope whose frequencies are proportional to the areas of the periodic orbits.

V. COMPARISON WITH NUMERICS AND EXPERIMENT

Since one of the main theoretical results of the present paper concerns the periodic modulation of the Coulomb blockade peak heights, it is natural to consider the Fourier power spectrum of $G_{\rm peak}(k)$. In Fig. 1 we present a comparison of the numerical and semiclassical power spectra, calculated for a chaotic (stadium) dot, for three different placements of the leads. The exact conductance peaks are obtained numerically from Eq. (1), with the eigenstates being constructed using the the method of Ref. 43. To observe the variation in peak height, we vary the energy, or equivalently the wave vector $k=p/\hbar$, which changes the number of electrons on the dot as more levels are filled. Previously, we reported the case for leads placed symmetrically, as in the upper plot of Fig. 1, and $kR=70$.[23]

The data clearly demonstrate that the power spectrum has well-defined peaks corresponding to periodic orbits. The numerical results for the symmetric leads show excellent agreement with the semiclassical prediction.

However, the situation is different for asymmetrically positioned leads when there is no single short periodic orbit connecting both leads. In this case, only the main peak corresponding to the first repetition of the relevant periodic orbits, the ''diameter'' and the V-shaped orbit, is adequately reproduced. The higher-frequency behavior, however, is substantially different from the semiclassical prediction. We attribute this difference to the nonlinear mixing of the oscillations of different partial widths, neglected in our derivation of Eq. (54). The pronounced peak at the difference length L_V-L_D, where L_V and L_D correspondingly represent the lengths of the V-shaped and diameter orbits, strongly indicates that, although semiclassically small, the mixing effects of higher order terms in Eq. (50) can be significant in the experimentally relevant parameter range. We numerically verified that the sum and difference lengths can be partially obtained by Eq. (50).

As follows from Eq. (61), the oscillatory component of the ''local average'' conductance and the height of the corresponding peak in the power spectrum depends nontrivially on the position and width of the lead. This dependence is illustrated in Fig. 2, where we plot the amplitude of the ''diameter'' orbit contribution to the conductance as a function of $ka_{\rm eff}$ extracted from numerical length spectrum and the corresponding semiclassical prediction.

In Fig. 3 we compare the semiclassical correlation function with numerical data for the stadium dot. The oscillatory behavior for large separations reflects the peak in the corresponding power spectrum in Fig. 1 and is in agreement with the semiclassical result. The positive correlation for nearest neighbors is also in agreement with the semiclassical theory, demonstrating the influence of dynamics even in this apparently nonsemiclassical regime.

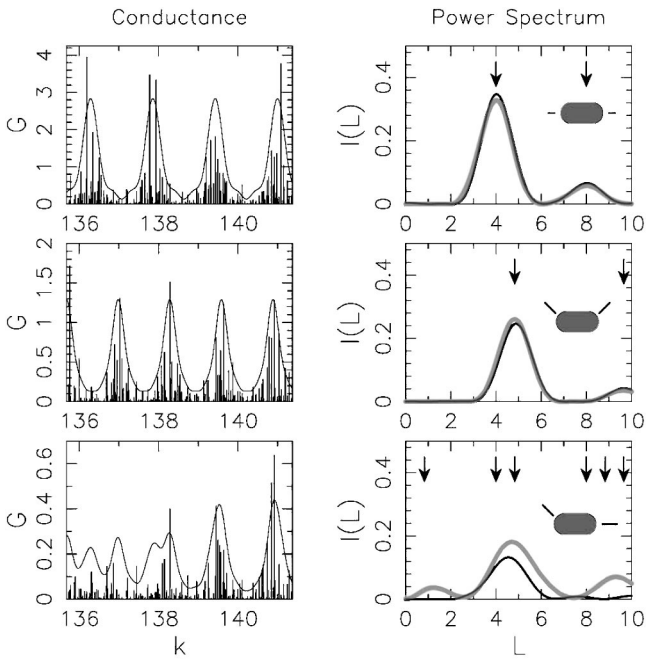

FIG. 1. The peak conductances (left column) from tunneling through subsequent energy levels in the stadium quantum dot and the corresponding ''length spectra'' $I(L)$ (right column) for different lead configurations (shown in the insets). In the peak conductance plots, each peak is placed at a wave vector k corresponding to its level; R is the radius of the half-circle parts of the stadium dot, and data for $kR\approx 140$ are shown. A Gaussian lead wave function appropriate for tunneling from a single transverse mode is used with width $ka_{\rm eff}=15$. The curves represent the semiclassical envelopes, defined by the contributions of the relevant periodic orbits (top: ''diameter'' orbit; middle: ''V''-shaped orbit; bottom: both diameter and V-shaped orbits). Length spectrum of the oscillations in $G(k)$ obtained from the Fourier power, numerical (thick gray line), and semiclassical (thin black line) results are compared. The power is normalized to the mean conductance. The arrows at the top show the positions of the relevant periodic orbits and their repetitions, as well as the ''combination lengths'' $L_1\pm L_2$. In the top panel, the peak at $L/R\simeq 4$ is the diameter, and that at 8 is its repetition. In the middle panel, the peak at $L/R=2(1+\sqrt{2})\approx 4.8$ corresponds to the V-shaped orbit, and the peak at $L/R\approx 9$ represents its repetition. In the bottom panel (asymmetric leads), the broad peak at $L/R\simeq 4.5$ represents the total contribution of both diameter- and *V*-shaped orbits. For the stadium dot, the principal peaks appear at 4 and 4.8, because we use only wave functions symmetric about the vertical and horizontal symmetry axes (equivalent to using only the even-even states of the stadium). Note the excellent agreement between the semiclassical theory and the numerical results for symmetric leads, and adequate representation of the principal peak for asymmetric leads.

When $T\gg\Delta$, the major source of correlations between neighboring peaks is the joint contribution of several resonances to the same conductance peak.[8] In this regime the

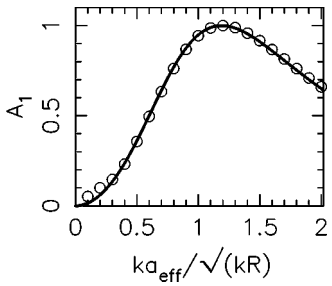

FIG. 2. The dependence of the amplitude of the length spectrum peak at $L/R \simeq 4$ on ka_{eff} for $kR=70$. The leads are symmetrically attached to the middle of the semicircle segments of the stadium dot.

''nearest-neighbor'' correlator is $\text{Corr}_{m=1} \sim 1$, and the dynamical effect accounts for only a small correction to the correlation function. However, for low temperature $T \leqslant \Delta$, the correlations due to temperature are exponentially suppressed. In this regime, as illustrated in Fig. 4, the correlations induced by dynamical modulation dominate, and they account for the experimentally observed enhancement of correlations at low temperatures.[9] For finite temperature each resonance is weighted by combinations of Fermi-Dirac functions and occupation numbers.[24] The occupation numbers used in Fig. 4 were obtained by employing a recursion relation;[44] see the Appendix. As the temperature increases more resonances contribute to a single conductance peak, and thus dampening the effects of the longer orbits.

In Fig. 5 we present the results of the calculation of the probability distribution of G_{peak} for a stadium quantum dot for both ''symmetric'' and ''asymmetric'' placements of the leads. For comparison, we show both the actual distribution [Eqs. (49) and (54)], and the standard Porter-Thomas result without any account of the modulation of the average conductance: $P(G_{\text{peak}})=\sqrt{4/\pi G_{\text{peak}}}\exp(-G_{\text{peak}})$. As the *individual* peak-height distribution is essentially a local measure, it is not strongly sensitive to the correlations, and both the standard and dynamical theories predict nearly the same result, and both are consistent with numerical calculation. This explains why no dynamical effect was observed in the experimental peak-height probability distribution.[6,7]

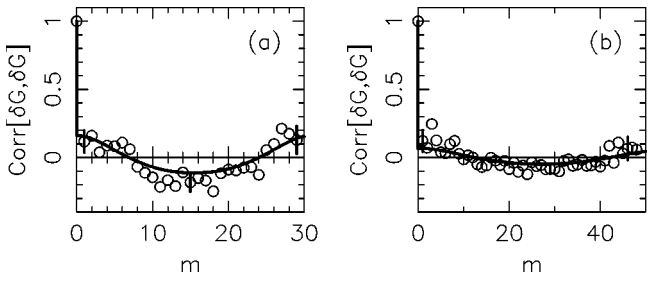

FIG. 3. The peak-to-peak conductance correlation function for (a) symmetrically placed leads (attached to the ''diameter'' of the stadium dot), and (b) asymmetric leads (as in the inset to the length spectrum at the bottom of Fig. 1). The numerical correlation function (circles with typical error bars)—the average of all pairs of peaks m peaks apart—is in good agreement with the semiclassical theory (solid line). The agreement for small m is surprising since this regime is not semiclassical, but shows how dynamics can give rise to correlations even between nearest neighbors. The difference between the periods of the modulation in (a) and (b) is accounted for by the difference in the values of kR used for the correlation function: the calculation for (a) is performed near $kR=70$, while (b) corresponds to an interval near $kR=140$.

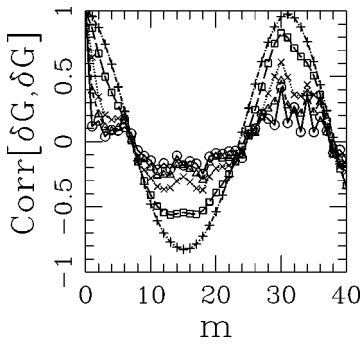

FIG. 4. The peak amplitude correlation function for a stadium-shaped dot with symmetrically attached leads and for temperatures $T=0$ (circles), 0.25Δ (triangles), 0.5Δ (X's), Δ (squares), and 2Δ (pluses), and $kR=70$. The solid, dashed, and dotted lines are only used to guide the eye.

In contrast, a periodic modulation of the peak heights was observed in several recent experiments.[7,9,22] The clearest observation is in Ref. 9: the data in their Fig. 1 showed modulated peak heights as a function of the number of electrons in the dot. In their trace of 90 peaks, approximately six oscillations are visible, yielding a period of ~ 15 peaks.

In our treatment, this period is related to the period of fundamental oscillation in Eq. (61). A variation in action ΔS_μ can arise in two different ways: either the Fermi momentum changes or the dynamics, that is the lengths of the periodic orbits, is modified. In general both effects will be present.

First, if only the momentum varies, then the fundamental period is given by $[(1/h)\partial S_\mu/\partial\varepsilon]^{-1} \equiv h/\tau_\mu$ where τ_μ is the period of the relevant orbit, and the ratio of this to the level spacing Δ gives the period of the peak heights. Note that

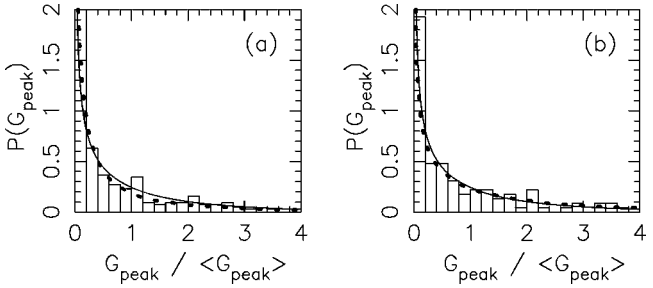

FIG. 5. Conductance statistics: probability distribution function for (a) symmetric leads at $kR=140$, and (b) asymmetrically placed leads at $kR=70$. The numerical probability distribution (histogram) is for the entire range of data in Fig. 1, and is compared to both the semiclassical theory (dotted line) and the standard statistical theory based on random wave functions (solid line). The two theories predict nearly the same result for this quantity (especially for asymmetric leads, where the dynamical modulation is weaker), and both are consistent with the numerics.

presenting the experimental data as the number of peaks per oscillation removes the effects of the charging energy: a constant shift of all the levels as an electron is added to the dot contributes to the peak spacing but not to the *number* of levels that need to be filled in order for the interference condition around a periodic orbit to change. In fact, small fluctuations in either the charging energy or the mean single-particle level spacing do not matter. In the billiard approximation, $\tau_\mu \equiv L_\mu / v_F$, where L_μ is the length of the periodic orbit and v_F is the Fermi velocity, which can be calculated from the experimental density.[45]. Using the appropriate spin-resolved level spacing $\Delta \simeq 10\ \mu$eV (which is half of the spin-full value from the measurements in Ref. 9) and the orbit from the lead to the ''pin'' gate and back (whose length we estimate to be $0.9\ \mu$m), we expect an oscillation period of ~ 75 peaks. This value is inconsistent with the experimental observation.[46]

Second, changes in the dynamics caused by a deformation[12] should also be considered. By examining the configuration of the dot in the inset of Fig. 1 of Ref. 9, the gate voltage appears to be situated on the shortest periodic orbit of each lead. By making the gate voltage more negative, the electron will have a shorter path and thus contribute to the change of the action in Eq. (61). If the Fermi energy of the system remains constant, then we can calculate a plausible range for the period using two extreme simplified models for the deformation of the boundary. First, the gate voltage is modeled as a small local semicircular deformation. Equating the area of the semicircle to the number of peaks times the change of area caused by adding one electron on the dot without a change in the Fermi energy, we estimate the period to be ~ 3 peaks independent of the Fermi energy. The other extreme is considering the entire side to move uniformly. The same procedure yields a period proportional to the square root of the number of electrons on the dot. Assuming that the typical dot in these experiments has 100 electrons,[9] we obtain a period of ~ 13 peaks. Since the true behavior of the gate is no doubt intermediate between these two extremes, we find that this mechanism acting by itself would produce a period of $\sim 5-10$ peaks.

A related possiblity is that the adding of electrons may change the effective potential defining the dot because of the added charge. This could be another source of a change in the dynamics. However, such a change in effective potential will not be localized near one of the periodic orbits, but will rather spread out across the quantum dot. In fact, experiments on ''magnetofingerprints'' of the peaks[47] suggest a certain robustness of the effective potential—its change from peak to peak seems to be small in this case. In contrast, to affect the dynamical modulation one must substantially change the action of the shortest periodic orbit, which typically requires a much larger change in potential such as could be caused by the external gates.

Thus, the experimental result of a period of 15 peaks cannot be solely obtained by either the orbit length change (too small) or the change in Fermi momentum (too large). A combination of these two effects, no doubt both present in real systems, yields an intermediate result consistent with experiment. Unfortunately, the range of possible periods that results from this simple modeling of the quantum dot is very broad, and so this is hardly a stringent test of the semiclassical theory. A detailed model of the confining potential and gate voltage effects is necessary in order to make a better prediction of the oscillation period.

A similar approach to the peak modulation as a function of magnetic field is also consistent with the experimental results,[7,22] where a quasiperiodic modulation of the peak heights was observed with a period $\Delta B \simeq 35$ mT. In our treatment, this period is given by the ratio of the flux quantum hc/e to the area $\mathcal{A}_0$ enclosed by the periodic orbit. From the experimental oscillation, we obtain $\mathcal{A}_0 \simeq 0.12\ \mu\text{m}^2$. This is consistent with the total area of the dot, $0.32\ \mu\text{m}^2$,[7] considering that there is likely to be some cancellation of fluxes between different parts of the orbit.

A puzzling feature of the initial experiments was that the dynamical modulation of the Coulomb blockade peak heights was not seen in the experiment of Ref. 6. We attribute this behavior to two factors: the positioning of the leads relative to the gate, and the relatively small mean free path. First, if the gate used to change the number of electrons is not along the shortest periodic orbit of either lead and the Fermi energy does not change appreciably in the dot, then one should not observe oscillations in the conductance peaks. In the geometry of Ref. 6, the leads and gate seem to be rather disconnected, so this is a factor. Second, in this experiment the mean free path $l \sim 0.4\ \mu$m only marginally exceeds the typical size of the dot $d \simeq 0.25\ \mu$m, while the length of the shortest periodic orbit is at least twice the effective ''diameter'' d of the dot: $L_{\min} > 2d \simeq 0.5\ \mu\text{m} > l$. If the mean free path is caused by short-range diffractive scattering, the dynamical effects are suppressed and will not affect the Coulomb blockade measurements. However, in the opposite limit of a smooth scattering potential, dynamical effects caused by coherent branched flow[48] may still be present. The short mean free path measured in Ref. 6 suggests the presence of impurities in the two-dimensional electron-gas layer, leading to a short-range scattering potential and so suppression of dynamical effects.

VI. SUMMARY

In conclusion, using semiclassical methods, we developed a dynamical statistical theory of Coulomb blockade peak heights in chaotic quantum dots. We derived the peak height distributions and the correlation functions, and showed that the corrections to the corresponding results of the standard statistical theory can be expressed in terms of the classical periodic orbits of the dot. Both our analytical results and numerical simulations clearly demonstrate that the dynamical effect is significant for both symmetric and asymmetric lead placements.

We close with two further experiments suggested by our results. First, if the tuning parameter used to change the number of electrons, such as a gate voltage, does not change the action of the dominant periodic orbit, then no modulation connected to that orbit should be seen. In particular, gates which affect different parts of the dot may produce different oscillatory behaviors. Second, several samples made in a ro-

bust geometry—a circle with directly opposite leads, for example—should show the same modulation. Any deviations from the same behavior would be a sensitive indication of the material quality.

ACKNOWLEDGMENTS

We gratefully acknowledge stadium eigenfunction calculations by J. H. Lefebvre, and helpful discussions with C. M. Marcus and M. Srednicki. We thank L. Kaplan for making available Ref. 35, which we received during the final stages of this work.

APPENDIX: TEMPERATURE CALCULATIONS

For nonzero temperatures the conductance is obtained from a weighted sum over the zero temperature partial widths Γ_λ.[24] For symmetric leads, this yields

$$G=\frac{e^2}{h}\frac{\pi}{4kT}\sum_\lambda w_\lambda\Gamma_\lambda . \tag{A1}$$

If $kT,\Delta\ll e^2/C$, then the weights are given by

$$w_\lambda=4f(\Delta F_{N_0}-\tilde{E}_F)\langle n_\lambda\rangle_{N_0}[1-f(E_\lambda(N)-\tilde{E}_F)], \tag{A2}$$

where ΔF_N is the change in the canonical free energy from $N-1$ to N, $\langle n_\lambda\rangle_N$ is the canonical occupation, $\tilde{E}_F=E_N+(N-1/2)e^2/C$ is an effective Fermi energy, and $f(\epsilon)=[1+\exp(\epsilon/kT)]^{-1}$ is the Fermi-Dirac function.

To obtain the canonical free energy and canonical occupation number we use a recurrence relation developed by Brack, Genzken, and Hansen[44] for the partition function $Z(N,M;\beta)$; N is the number of particles, M is the number of levels, and $\beta=1/kT$. The final result for the partition function will not numerically depend upon M for large M. The partition function is formally given by

$$Z(N,M;\beta)\equiv\sum_{\alpha=1}^{I_{NM}}\exp(-\beta E_\alpha(N))=\exp(-\beta E_0)z(N,M;\beta), \tag{A3}$$

where

$$z(N,M;\beta)\equiv\sum_{\alpha=1}^{I_{NM}}\exp(-\beta[E_\alpha(N)-E_0]). \tag{A4}$$

Here $E_\alpha(N)$ is the sum of the energy of the single-particle occupied levels ϵ_M which does not include the charging energy; E_0 will be defined below, and I_{NM} is the number of ways to fill M levels with N identical particles. The recurrence relation derived in Ref. 44 is

$$\begin{aligned}Z(N,M;\beta)&=Z(N,M-1;\beta)\\&\quad+\exp(-\beta\epsilon_M)Z(N-1,M-1;\beta)\\&\quad\text{for}\quad N\geqslant 1,M\geqslant N,\end{aligned} \tag{A5}$$

with the constraints

$$Z(0,M;\beta)\equiv 1\quad\forall M\geqslant 0, \tag{A6}$$

$$Z(N,N-1;\beta)\equiv 0\quad\forall N\geqslant 1. \tag{A7}$$

Note that the same recurrence relation also holds for $z(N,M;\beta)$. The choice $E_0(N)=\Sigma_{m=1}^{N}\epsilon_m$ yields the result

$$z(N,N;\beta)=1. \tag{A8}$$

Using conditions (A7) and (A8) as starting points for the recurrence relation [Eq. (A5)], we obtain $z(N,M\to\infty;\beta)$ and thus $Z(N,M\to\infty;\beta)$. For the small temperatures that we consider, the convergence of the recurrence relation is rapid.

Similarly, one can calculate a modified partition function $Z'_\lambda(N,M;\beta)$ which has level λ removed from the spectrum. The probability for level λ to be unoccupied, $P\{n_\lambda=0\}$, is, then, simply Z'_λ/Z. In terms of this probability, the average occupation numbers are given by $\langle n_\lambda\rangle_N=1-P\{n_\lambda=0\}$. Finally, the canonical free energy for N electrons, $F(N)$, appearing in Eq. (A2), is

$$F(N)=-\frac{1}{\beta}\ln Z(N,M\to\infty;\beta). \tag{A9}$$

[1] H. Grabert and M.H. Devoret, *Single Charge Tunneling: Coulomb Blockade Phenomena in Nanostructures* (Plenum Press, New York, 1992).

[2] R.A. Jalabert, A.D. Stone, and Y. Alhassid, Phys. Rev. Lett. **68**, 3468 (1992).

[3] L P. Kouwenhoven, C.M. Marcus, P.L. McEuen, S. Tarucha, R.M. Westervelt, and N.S. Wingreen, in *Mesoscopic Electron Transport*, edited by L.L. Sohn, L.P. Kouwenhoven, and G. Schön (Kluwer, Dordrecht, 1997), pp. 105–214.

[4] Y. Alhassid, Rev. Mod. Phys. **72**, 895 (2000).

[5] M. Stopa, Physica B **251**, 228 (1998).

[6] A.M. Chang, H.U. Baranger, L.N. Pfeiffer, K.W. West, and T.Y. Chang, Phys. Rev. Lett. **76**, 1695 (1996).

[7] J.A. Folk, S.R. Patel, S.F. Godijn, A.G. Huibers, S.M. Cronenwett, and C.M. Marcus, Phys. Rev. Lett. **76**, 1699 (1996).

[8] Y. Alhassid, M. Gökçedag, and A.D. Stone, Phys. Rev. B **58**, 7524 (1998).

[9] S.R. Patel, D.R. Stewart, C.M. Marcus, M. Gökçedag, Y. Alhassid, A.D. Stone, C.I. Duruöz, and J.S. Harris, Jr., Phys. Rev. Lett. **81**, 5900 (1998).

[10] M. Stopa, Phys. Rev. B **54**, 13 767 (1996).

[11] G. Hackenbroich, W.D. Heiss, and H.A. Weidenmüller, Phys. Rev. Lett. **79**, 127 (1997).

[12] R.O. Vallejos, C.H. Lewenkopf, and E.R. Mucciolo, Phys. Rev. B **60**, 13 682 (1999).

[13] M. Gutzwiller, *Chaos in Classical and Quantum Mechanics* (Springer, New York, 1990).

[14] J.B. Delos and C.D. Schwieters, in *Classical, Semiclassical and*

Quantum Dynamics in Atoms, edited by H. Friedrich and B. Eckhardt (Springer, Berlin, 1997), pp. 223–247; M.W. Beims, V. Kondratovich, and J.B. Delos, Phys. Rev. Lett. **81**, 4537 (1998).
[15] E.J. Heller, in *Chaos and Quantum Physics*, edited by M.J. Giannoni, A. Voros, and J. Zinn-Justin (Elsevier, Amsterdam, 1991), pp. 547–663.
[16] L. Kaplan, Phys. Rev. Lett. **80**, 2582 (1998); L. Kaplan and E.J. Heller, Ann. Phys. (N.Y.) **264**, 171 (1998).
[17] D. Weiss, K. Richter, A. Menschig, R. Bergmann, H. Schweizer, K. von Klitzing, and G. Weimann, Phys. Rev. Lett. **70**, 4118 (1993); G. Hackenbroich and F. von Oppen, Europhys. Lett. **29**, 151 (1995); K. Richter, *ibid.* **29**, 7 (1995).
[18] E.E. Narimanov, A.D. Stone, and G.S. Boebinger, Phys. Rev. Lett. **80**, 4024 (1998); an alternative semiclassical theory of resonant magnetotunneling was developed by E.B. Bogomolny and D.C. Rouben, Europhys. Lett. **43**, 111 (1998).
[19] T.S. Monteiro, D. Delande, A.J. Fisher, and G.S. Boebinger, Phys. Rev. B **56**, 3913 (1997).
[20] D. Saraga and T.S. Monteiro, Phys. Rev. Lett. **81**, 5796 (1998).
[21] E.E. Narimanov and A.D. Stone, Physica D **131**, 220 (1999).
[22] S.M. Cronenwett, S.R. Patel, C.M. Marcus, K. Campman, and A.G. Gossard, Phys. Rev. Lett. **79**, 2312 (1997).
[23] E.E. Narimanov, N.R. Cerruti, H.U. Baranger, and S. Tomsovic, Phys. Rev. Lett. **83**, 2640 (1999).
[24] C.W.J. Beenakker, Phys. Rev. B **44**, 1646 (1991).
[25] J. Bardeen, Phys. Rev. Lett. **6**, 57 (1961).
[26] M.V. Berry, Phys. Rev. Lett. **10**, 2083 (1977); for a description of the properties of random functions, also see P.W. O'Connor, J. Gehlen, and E.J. Heller, *ibid.* **58**, 1296 (1987).
[27] Y. Alhassid and C.H. Lewenkopf, Phys. Rev. Lett. **75**, 3922 (1995).
[28] M. Srednicki, Phys. Rev. E **54**, 954 (1996).
[29] V.N. Prigodin, K.B. Efetov, and S. Idia, Phys. Rev. Lett. **71**, 1230 (1993).
[30] V.N. Prigodin, B.L. Altshuler, K.B. Efetov, and S. Idia, Phys. Rev. Lett. **72**, 546 (1994).
[31] V.N. Prigodin, Phys. Rev. Lett. **74**, 1566 (1995).
[32] V.N. Prigodin, N. Taniguchi, A. Kudrolli, V. Kidambi, and S. Sridhar, Phys. Rev. Lett. **75**, 2392 (1995).
[33] M. Srednicki and F. Stiernelof, J. Phys. A **29**, 5817 (1996).
[34] S. Hortikar and M. Srednicki, Phys. Rev. Lett. **80**, 1646 (1998).
[35] L. Kaplan, Phys. Rev. E **62**, 3476 (2000); [arXiv:nlin.CD/0003013 (unpublished)].
[36] C. Jarzynski, Phys. Rev. E **56**, 2254 (1997).
[37] C.E. Shannon, Bell Syst. Tech. J. **27**, 379 (1948); **27**, 623 (1948).
[38] M. Brack and R.K. Bhaduri, *Semiclassical Physics* (Addison-Wesley, New York, 1997).
[39] P.W. Brouwer, Y. Oreg, and B.I. Halperin, Phys. Rev. B **60**, R13 977 (1999).
[40] H.U. Baranger, D. Ullmo, and L.I. Glazman, Phys. Rev. B **61**, R2425 (2000).
[41] D. Ullmo and H.U. Baranger, cond-mat/0103098 (unpublished).
[42] M. Srednicki (private communication).
[43] T. Szeredi, J.H. Lefebvre, and D.A. Goodings, Nonlinearity **7**, 1463 (1994).
[44] M. Brack, O. Genzken, and K. Hansen, Z. Phys. D: At., Mol. Clusters **21**, 65 (1991).
[45] C. M. Marcus (private communication).
[46] This estimate and conclusion contradict that in our previous publication (Ref. 23), which we now believe to be missing a factor of 2π in the definition of the fundamental period and a factor of 2 due to single bounce orbits. The result is an overall factor of π that arises when comparing the formulas in Ref. 23 (which are correctly given) to the experiments.
[47] D.R. Stewart, D. Sprinzak, C.M. Marcus, C.I. Duruöz, and J.S. Harris, Science **278**, 1784 (1997).
[48] M.A. Topinka, B.J. LeRoy, R.M. Westervelt, S.E.J. Shaw, R. Fleischmann, E.J. Heller, K.D. Maranowski, and A.C. Gossard, Nature (London) **410**, 183 (2001); [arXiv:cond-mat/0010348] (unpublished); also see M.A. Wolfson and S. Tomsovic, J. Acoust. Soc. Am. **105**, 1116 (1999) and (to be published); [arXiv:nlin.CD/0002030 (unpublished)].